The EMBO Journal Vol.17 No.4 pp.1169–1181, 1998

Efficient transposition of IS*911* circles *in vitro*

B.Ton-Hoang, P.Polard and M.Chandler[1]

Laboratoire de Microbiologie et Génétique Moléculaire du CNRS, 118 Route de Narbonne, 31062 Toulouse, France

[1]Corresponding author
e-mail: mike@ibcg.biotoul.fr

An *in vitro* system has been developed which supports efficient integration of transposon circles derived from the bacterial insertion sequence IS*911*. Using relatively pure preparations of IS*911*-encoded proteins it has been demonstrated that integration into a suitable target required both the transposase, OrfAB, a fusion protein produced by translational frameshifting between two consecutive open reading frames, *orf*A and *orf*B, and OrfA, a protein synthesized independently from the upstream *orf*A. Intermolecular reaction products were identified in which one or both transposon ends were used. The reaction also generated various intramolecular transposition products including adjacent deletions and inversions. The circle junction, composed of abutted left and right IS ends, retained efficient integration activity when carried on a linear donor molecule, demonstrating that supercoiling in the donor molecule is not necessary for the reaction. Both two-ended integration and a lower level of single-ended insertions were observed under these conditions. The frequency of these events depended on the spacing between the transposon ends. Two-ended insertion was most efficient with a natural spacing of 3 bp. These results demonstrate that transposon circles can act as intermediates in IS*911* transposition and provide evidence for collaboration between the two major IS*911*-encoded proteins, OrfA and OrfAB.

Keywords: insertion sequence/IS*911*/transposition

Introduction

Studies on well-known bacterial transposons such as bacteriophage Mu, Tn*7* and IS*10 in vitro* have shown that their transposases cleave the ends of their cognate elements in different ways. Cleavage occurs either (i) on only one DNA strand at both ends, liberating two 3′ transposon ends while retaining linkage with the donor backbone via the 5′ ends [e.g. Mu; see Mizuuchi (1992a,b) for review], or (ii) on both strands at both ends, resulting in physical separation from the donor backbone [e.g. IS*10* and Tn*7*; for reviews see Craig (1996) and Kleckner *et al.* (1996)]. In both cases, the uncovered 3′-OH groups of the transposon then act as nucleophiles which attack the phosphodiester backbone of the target DNA in a subsequent strand-transfer reaction. In the first case, a branched 'Shapiro' intermediate is formed which, upon replication of the element, generates a cointegrate molecule where donor and target DNA are joined by two directly repeated copies of the transposon, one at each junction. In the second case, a simple insertion (without replication) of the element is obtained.

There are over 500 known bacterial insertion sequences, nearly 20% of which are members of the IS*3* family which has members in over 40 bacterial species (J.Mahillon and M.Chandler, submitted). Only limited information is available concerning the mechanism of transposition of IS*3* family members. Studies with one member, IS*911*, have suggested that its transposition strategy may differ from those described previously and implicate a circularized transposon as an intermediate (Ton-Hoang *et al.*, 1997).

IS*911* transposase, OrfAB, is a fusion protein assembled from two consecutive, partially overlapping reading frames, *orf*A and *orf*AB, by translational frameshifting (see Chandler and Fayet, 1993). When an IS*911*-carrying plasmid is supplied with elevated levels of this protein *in vivo*, it gives rise to two prominent novel molecules. One is a figure-of-eight form in which a single transposon strand is circularized retaining both terminal inverted repeats (IR) in a single-stranded bridge. The bridge is composed of abutted left (IRL) and right (IRR) ends separated by three bases which originally flanked one or other end in the donor molecule (Polard and Chandler, 1995). The second species is a transposon circle in which the second transposon strand has also been joined (Polard *et al.*, 1992). Such circular forms have been observed for several other members of the IS*3* family: IS*3* itself (Sekine *et al.*, 1994) and IS*150* (Welz, 1993), while both circular and figure-of-eight forms have been observed with IS*2* (Lewis and Grindley, 1997).

It has been suggested that circle formation is a two-step process with the figure-of-eight molecule as a precursor. Kinetic data are consistent with this notion (Polard and Chandler, 1995; G.Duval-Valentin, unpublished results). However, several lines of evidence suggest that the second transposon strand may not be cleaved and transferred by the same mechanism as the first. OrfAB appears to catalyse cleavage and transfer of only a single DNA strand *in vitro* (Polard *et al.*, 1996) and no evidence for double-strand cuts at the ends of IS*911* has yet been obtained. In addition, no transposon circles are generated in an *in vitro* system which faithfully and efficiently reproduces figure-of-eight formation. 'Resolution' of the second strand to generate circles from the figure-of-eight form was proposed to require a host function (Polard *et al.*, 1996; Ton-Hoang *et al.*, 1997).

Further support for the idea that the second strand is processed in a different way from the first comes from the apparent asymmetry of strand transfer in both the figure-of-eight and circle. Like the figure-of-eight joint, the left and right IS*911* terminal inverted repeats, IRL and

IRR, in the circle junction are abutted and separated by three base pairs originally flanking one or other end in the donor molecule (Polard *et al.*, 1992). Mutation of the terminal 5′-CA-3′ at both ends abolishes figure-of-eight and circle formation *in vivo*, indicating an essential role for this dinucleotide. Mutation of one end, however, has no apparent affect on either figure-of-eight or circle formation (Polard and Chandler, 1995; Polard *et al*., 1992, 1996). In these cases, the wild-type end is transferred exclusively to the mutant end and the three intervening bases in both the figure-of-eight and circle junctions are uniquely those originally attached to the mutant end (Polard and Chandler, 1995). This has also been observed more recently with IS*2*, which has a naturally 'inactive' left end (Lewis and Grindley, 1997).

Assembly of the IS*911* circle junction generates a strong promoter, p_{JUNC}, in which a –35 hexamer is contributed by IRR and a –10 hexamer by IRL. This promoter is significantly stronger than the indigenous promoter, p_{IRL}, and, moreover, is correctly placed to drive high levels of transposase synthesis (Ton-Hoang *et al.*, 1997). These observations have suggested a model for IS*911* transposition in which circularization and assembly of p_{JUNC} lead to high levels of transposition proteins. Transposase can then act efficiently at the circle junction, introducing single-strand cleavages at the 3′ end of each abutted IR. The activated 3′-OH groups then act as donors in a concerted strand transfer to a suitable target DNA molecule. Cleavage and insertion would destroy p_{JUNC} and reduce transposase synthesis to a basal level. Thus high levels of transposition proteins would be produced only in response to the presence of a suitable substrate: the transposon circle. The idea that IS*911* circles are intermediates in transposition was supported by the demonstration that the circle junction is highly active in integration *in vivo*, and that excision in the form of circles could be detected with natural transposase levels (Ton-Hoang *et al.*, 1997). These experiments also suggested that, while OrfAB alone was sufficient to promote efficient circle formation, insertion was strongly stimulated by the simultaneous presence of OrfA, the product of the upstream *orf*A. OrfA has also been shown to stimulate OrfAB-mediated intermolecular transposition *in vivo*, in a mating-out transposition assay (Polard *et al.*, 1992).

To assess the role of transposon circles in IS*911* transposition, to determine the mechanism of circle integration and to define the roles of both OrfA and OrfAB in the process, it is essential to develop an *in vitro* recombination system. Such a system would also facilitate definition of the cleavage and strand-transfer reactions involved and provide access to study of the higher-order DNA–protein complexes which presumably need to be assembled during transposition. In the results presented here we describe an *in vitro* system which supports efficient inter- and intramolecular transposition of IS*911* circles. Intermolecular transposition resulted in molecules in which insertion used both ends or, at a lower level, only a single transposon end. Intramolecular transposition generated a majority of adjacent deletions. We also show that the IRL–IRR junction retains efficient integration activity when carried by a linearized substrate. Thus supercoiling in the donor molecule is not necessary for the reaction. The pattern of these events depended on the spacing between the transposon ends. Two-ended integration was most efficient with a natural spacing of 3 bp. Moreover, OrfAB alone was found to promote a majority of one-ended integration events but addition of OrfA was found both to stimulate one-ended integration and dramatically increase two-ended integration. These observations therefore provide evidence for collaboration between the two major IS*911*-encoded proteins, OrfA and OrfAB.

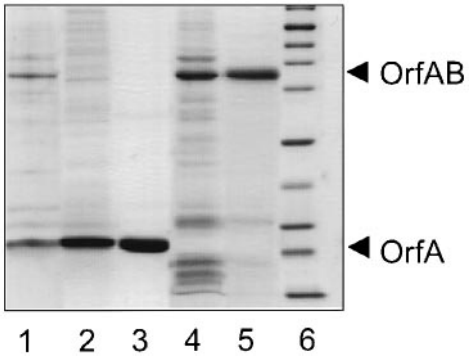

Fig. 1. Purification of IS*911*-encoded proteins. Coomassie-stained SDS/15% polyacrylamide gel showing purification steps. The right-hand lane shows standard molecular mass markers (6.5, 14.3, 20.0, 26.6, 36.5, 42.7, 55.6, 66.4, 97.2 and 116 kDa). Lane 1, WT preparation after the heparin–Sepharose step; lanes 2 and 3, enriched OrfA (30% ammonium sulfate precipitation and washing in low salt buffer) and after the heparin–Sepharose step respectively; lanes 4 and 5, enriched OrfAB (40% ammonium sulfate precipitation) and after the heparin–Sepharose step respectively. The positions of OrfA, OrfAB are indicated by arrowheads.

Results

Integration of IS911 circles in a cell-free system

IS911-encoded proteins and the integration substrate. The wild-type complement of IS*911* proteins (Figure 1, lane 1), OrfA (lane 3) and OrfAB (lane 5) were purified from cultures of strains harbouring plasmids pAPT155, pAPT156 and pAPT158 (Materials and methods). The plasmids carry, respectively: the wild-type *orf* configuration (in which OrfAB is naturally produced by –1 programmed translational frameshifting), *orf*A and *orf*AB (where *orf*A and *orf*B are fused by mutation) (Polard *et al*., 1996). These genes are under the control of p_{lacUV5} and the ribosome-binding site of the Φ10 gene of phage T7.

The substrates used were transposon circles produced *in vivo* with a two-plasmid system in which one plasmid (pAPT111) serves as a source of OrfAB and the other (pAPT99) carries an IS*911*-based transposon in which copies of IRL and IRR flank a gene conferring resistance to chloramphenicol. After overnight induction of OrfAB expression, plasmid DNA was prepared by alkaline lysis. The circles of 3.8 kb were purified by agarose gel electrophoresis (Materials and methods).

Biological integration assay. The initial biological assay used a 7 kb supercoiled pBR322-based plasmid, pDAG92, as a target (Materials and methods). Substrate, target and IS*911*-encoded proteins were incubated in the reaction buffer with Mg^{2+} for 1 h at 30°C. The reaction mixture was deproteinized and used to transform a *rec*A derivative of MC1061 with selection for chloramphenicol resistance (Cm^R; transposon) or ampicillin resistance (Ap^R; target plasmid). Since transposon circles do not carry an origin

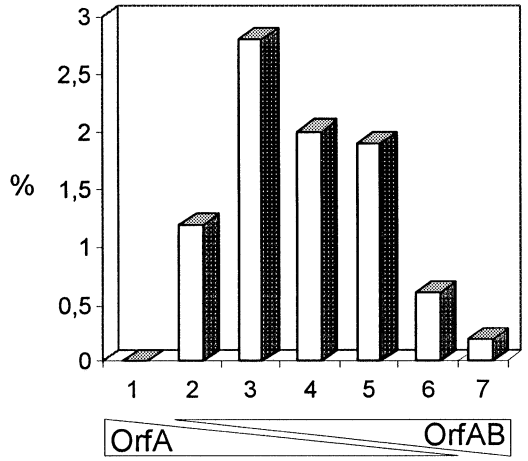

Fig. 2. Frequency of integration of transposon circles *in vitro* in a standard biological assay as a function of the OrfA/OrfAB ratio. The efficiency of transposition is expressed as the number of Cm^R transformants as a percentage of total (Ap^R) transformants. Different ratios of proteins OrfA and OrfAB were preincubated for 1 h at 4°C before addition to the reaction mixture in the presence of Mg^{2+} and DMSO with 50 ng of wild-type circle substrate (IRL^+/IRR^+) and 600 ng of pDAG92 as target. Lane 1, 1.08 μg OrfA; lane 2, 0.48 μg OrfAB and 0.90 μg OrfA; lane 3, 0.96 μg OrfAB and 0.72 μg OrfA; lane 4, 1.44 μg OrfAB and 0.54 μg OrfA; lane 5, 1.92 μg OrfAB and 0.36 μg OrfA; lane 6, 2.4 μg OrfAB and 0.18 μg OrfA; lane 7, 2.88 μg OrfAB. Note that 1 μg of OrfAB and of OrfA correspond to 22.5 pmol and 90 pmol respectively. The molar ratios of OrfA/OrfAB in lanes 2–6 are therefore 8:1, 3:1, 1.5:1, 1:1.3, 1:3.3 respectively.

of replication, acquisition of Cm^R is expected to depend on integration of the circle into pDAG92. The plasmid content of these Cm^R transformants was examined by digestion with suitable restriction enzymes. All carried a plasmid of a size and restriction pattern consistent with the insertion of a single transposon circle into pDAG92 (data not shown). Determination of the nucleotide sequence across the IS*911* ends of 10 independent clones confirmed that they were used in integrating the transposon and demonstrated that integration generated a direct target repeat of 3 bp characteristic of IS*911* simple insertion (Prère *et al.*, 1990) in nine of the 10 cases. The remaining insertion generated only a 2 bp direct target repeat. Thus, *in vitro*, the circle substrates incubated with IS*911* proteins gave rise to transposition products similar to those obtained *in vivo* with the 'natural' element.

The protein preparation obtained using the wild-type configuration of Orfs, WT, was significantly more efficient in the integration reaction with the wild-type circle substrate, IRL^+/IRR^+, than was OrfAB alone. For the same quantity of total protein, WT yielded a 50-fold higher ratio of Cm^R/Ap^R transformants than OrfAB (1% compared with 0.02%), even though the quantity of transposase in WT preparation is several times lower than in reactions with OrfAB alone (Figure 1, lanes 1 and 5).

The conditions were therefore initially modified to maximize reaction efficiency using the more active WT protein preparation. Substitution of Mg^{2+} by Mn^{2+} was found to double the activity while addition of dimethylsulfoxide (DMSO) stimulated the reaction three-fold. Ficoll, polyethylene glycol and polyvinyl alcohol did not stimulate integration. The reaction did not require an exogenous energy source and was inhibited by high salt. The standard reaction mixture contained 25 mM HEPES (pH 7.5), 0.3 M KCl, 10 mM $MgCl_2$, 10% DMSO, 2 mM dithiothreitol, 20 ng/ml bovine serum albumin (BSA), 14% glycerol, 600 ng of target DNA, 50 ng of circle substrate and 900 ng of WT protein in a 30 μl total reaction volume. The resulting molar ratio of substrate to target DNA was 1:6. The Cm^R transformants were obtained at frequency of about 5% per target molecule (Ap^R clones).

To confirm that the reaction reflected true transposition, the activity of a circle substrate in which IRL had been inactivated by mutation of the terminal 5′-CA-3′ dinucleotide (pAPT177; IRL^-/IRR^+) was assessed (Polard *et al.*, 1992, Ton-Hoang *et al.*, 1997). In the 'standard' *in vitro* assay the relative efficiency of integration was significantly reduced (0.4% compared with 5% obtained with the wild-type substrate). The nucleotide sequence of the junctions of several of these insertions revealed that integration occurred at the correct (but mutant) position at each transposon end (data not shown).

Stimulatory effect of OrfA. The increased efficiency of integration with WT proteins compared with OrfAB alone has previously been observed *in vivo* (Ton-Hoang *et al.*, 1997). Moreover, in the presence of OrfAB, OrfA has been shown to stimulate intermolecular transposition of IS*911* (Polard *et al.*, 1992). To analyse the stimulatory activity of OrfA in more detail, OrfA and OrfAB preparations were mixed in various ratios and the effect on integration efficiency was assessed. A preincubation of OrfA with OrfAB (4°C for 1 h) before addition to the reaction mixture was included since it was found to increase recombination activity several-fold. Addition of low quantities of OrfA (Figure 2, compare lanes 5 and 6 with 7) increased the yield of Cm^R transformants. Furthermore, the results shown in Figure 2 indicate that the efficiency of integration depended on the quantity of the transposase OrfAB and on the ratio of the two proteins. This result was confirmed in experiments in which OrfAB was maintained at a constant level while OrfA was varied (data not shown and see later). Addition of extract enriched in OrfB (Polard *et al.*, 1996) did not influence the yield (data not shown).

Physical assay of integration product

The biological assay described above permits rapid detection of final integration products in which two-ended integration of both transposon ends has occurred. It does not, however, permit detection of intermediate species and might not reveal other species which fail to give rise to productive transposition. To visualize other possible species, reaction products were examined following separation by agarose gel electrophoresis and detection by ethidium bromide staining and by Southern analysis using a probe specific for the circle substrate. The results are presented in Figure 3. In a reaction including WT protein but not the target pDAG92 DNA (lane 2), the transposon circle substrate (lane 1) gave rise to several supplementary bands of low electrophoretic mobility (β). In addition, a series of bands and a poorly defined smear (indicated collectively as α) migrated ahead of the open circular form of the substrate. Inclusion of target plasmid resulted in the appearance of three additional prominent higher molecular size bands (I–III) (lanes 3–5) together with several less prominent species and a smear of lower electrophoretic mobility (indicated collectively as γ).

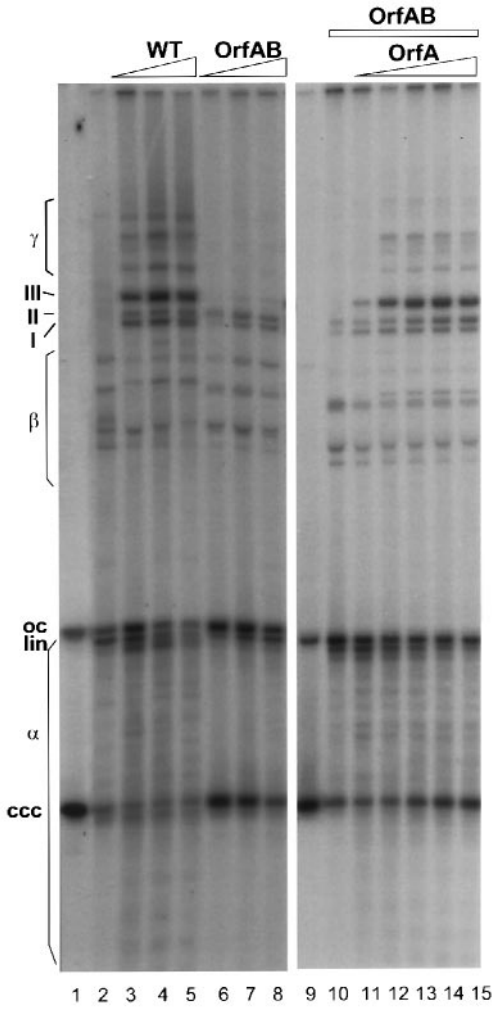

Fig. 3. Physical assay of integration reactions with a wild-type transposon circle substrate. Southern blot of integration reaction products performed under standard conditions (Materials and methods), separated on a 0.7% agarose gel (TAE buffer) and using oligonucleotide B21 as a probe. Lane 1, transposon circle substrate alone; lane 2, reaction carried out with 0.3 μg of WT protein preparation without target DNA. Plasmid pDAG92 was included as target DNA in all other lanes. Lanes 3–5: reactions with, 0.3, 0.9 and 1.8 μg of WT protein respectively; lanes 6–8, 0.48, 1.44 and 2.88 μg OrfAB. Lane 9, 0.54 μg OrfA; lanes 10–15, 0.48 μg OrfAB alone (lane 10) or with 0.18, 0.36, 0.54, 0.72 and 0.90 μg OrfA respectively (corresponding to molar ratios of OrfA/OrfAB 1.5:1, 3:1, 4.5:1, 6:1 and 8:1 in lanes 11–15 respectively). 'ccc', 'lin' and 'oc' indicate the supercoiled, linear and open circular forms respectively of the transposon circle substrate; α: intramolecular transposition products; β: autointegration products, I, II, III: major intermolecular transposition species; γ: higher molecular weight species.

Bands I–III hybridize with a probe specific for the target plasmid, demonstrating that they are intermolecular integration products (data not shown).

When compared with the profile obtained with WT protein (lanes 3–5), that obtained with OrfAB alone (lanes 6–8) lacked one major intermolecular band (III) and exhibited reduced levels of the other two (I and II). Band III was restored when OrfA was preincubated with OrfAB before addition of the protein mixture (lanes 10–15). Note that OrfA alone had no effect (lane 9). The relative intensity of band III varied as a function of the OrfA/OrfAB ratio and was correlated with the frequency of Cm^R transformants in the biological assay (data not shown). This suggests that band III reflects productive intermolecular transposition. The intensity of this band decreased in reactions containing higher levels of OrfA (data not shown). Species I and II, although present at low levels with OrfAB alone, are also increased in the presence of OrfA (compare lanes 10–15). Note that, compared with that obtained with WT, the profile of the α group of bands was simplified in the presence of OrfAB alone (compare lanes 3–5 and 6–8) but was partly restored upon addition of OrfA (lanes 10–15).

Identification of the principal species generated in vitro

Intermolecular integration: species I, II and III. In addition to products resulting from transfer of both transposon ends into the target molecule (Figure 4, species C), products resulting from transfer of a single end might also be expected. These could arise either by cleavage of a single transposon strand and transfer to generate a 'figure-of-eight' molecule (Figure 4, species B), or by cleavage of both strands of the circle junction to generate a 'linear' transposon and transfer of a single end to generate a σ form (Figure 4, species A). Cleavage of the second transposon strand of a figure-of-eight form without accompanying strand transfer would also generate a σ structure. In each case two types of molecule would be expected, depending on which end of the transposon has undergone strand transfer.

Species I, II and III were purified from the gel and used to transform a suitable recipient strain. Species III gave rise to Cm^R colonies whereas species I and II did not. The plasmid content of the Cm^R clones exhibited a size and restriction pattern consistent with a simple transposon insertion into pDAG92 (data not shown). Species III comigrated with the relaxed form of the plasmid obtained from Cm^R transformants in the original biological assay (data not shown), suggesting that it results from direct insertion of the transposon into pDAG92. This is the result expected for transfer of both 3′ transposon ends into target DNA *in vitro* which should occur in a staggered fashion generating three-base, single-stranded gaps in the vector flanking the 5′ transposon ends and resulting in a relaxed circular product (it would also leave three-base single-stranded 'tails' attached to the 5′ transposon ends; Figure 4, species C).

To examine its structure in more detail, species III was digested *in situ* in a gel slice with *Pst*I, which cleaves once within the target plasmid, or with *Sma*I, which cleaves within both target and transposon sequences. The products were visualized by electrophoresis in a second agarose gel and Southern hybridization with an oligonucleotide probe specific for the transposon (note that the probe hybridizes to both ends of the transposon and that *Sma*I cleaves almost exactly at the centre of the transposon). Digestion with *Pst*I generated a single band (arrowhead in Figure 4III, lane P) which migrated as a linear plasmid carrying a simple transposon insertion (Figure 4III, lane TP). Digestion with *Sma*I resulted in a smear of material (bracket in Figure 4III, lane S) presumably reflecting a population of molecules in which integration of a single transposon circle into a single target plasmid has occurred at many different sites.

Similarly, bands I and II were digested *in situ* with

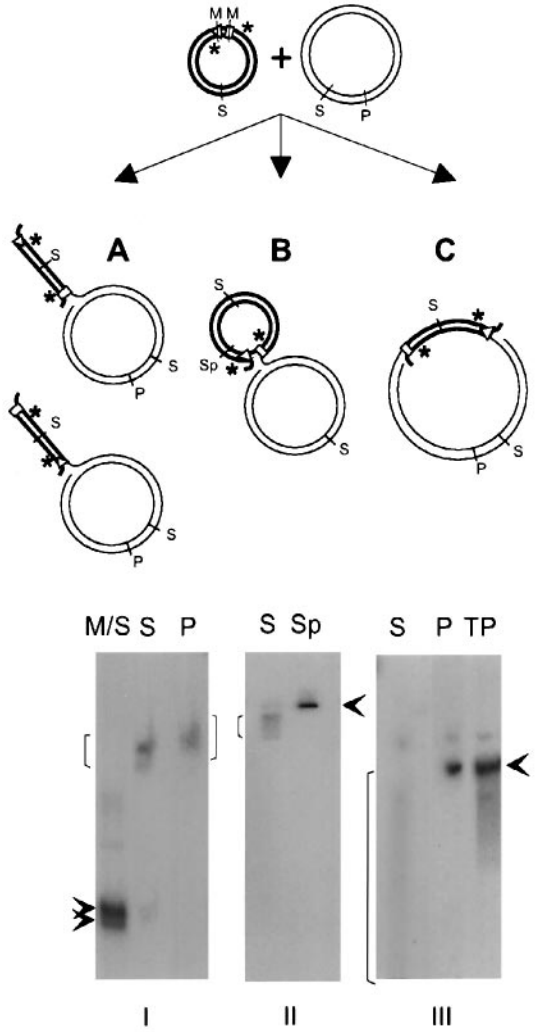

Fig. 4. Identification of major intermolecular transposition species I, II and III. The predicted structures of IS*911 in vitro* integration products are shown in the upper panel. A and B represent one-ended integration species while C represents a two-ended integration event. S, P, Sp and M indicate the location of sites for the restriction enzymes *Sma*I, *Pst*I, *Sph*I and *Msc*I respectively. Note that although the *Sph*I site is present in all three structures, it is shown only in B since the enzyme was only used in analysis of this form. * indicates the regions with homology to the oligonucleotide probe. The transposon is represented in bold and target DNA drawn as a fine line. The left (IRL) and right (IRR) terminal inverted repeats are shown as a box and a triangle respectively. The lower panels (I, II and III) present an analysis of forms I, II and III respectively by *in situ* digestion and Southern blotting. Bands corresponding to respective species were isolated from an ethidium bromide-stained agarose gel and digested *in situ* with different restriction enzymes prior to electrophoresis in a 0.7% agarose gel and probing with oligonucleotide B21. Lane M/S shows the results of digestion of purified transposon circles with *Msc*I (which cleaves once within each terminal IR) and *Sma*I. Lane TP shows the results of digestion by *Pst*I of DNA isolated from a Cm^R transformant. Lanes S, P, and Sp represent digestion of the relevant species with *Sma*I, *Pst*I and *Sph*I respectively.

*Sma*I, *Pst*I or *Sph*I (Figure 4I and II). As predicted for a figure-of-eight molecule, treatment of band II with *Sph*I generated a discrete band (arrowhead in Figure 4II, lane Sp). This should correspond to an α structure with a single cleavage in the transposon moiety. Digestion with *Sma*I should generate a family of χ structures since, in the population, the transposon would have inserted at various distances from the *Sma*I site in the target molecule. As predicted, this yielded a population which migrated as a high molecular size smear (bracket in Figure 4II, lane S). Digestion with *Pst*I (which cleaves once within pDAG92) to generate an equivalent α structure also gave rise to a high molecular weight smear (data not shown). Digestion of a σ form with *Sma*I would liberate a doublet derived from two reciprocal transposon fragments (Figure 4I, lane S), migrating at almost the same level as linear transposon digested with *Sma*I (arrowheads in Figure 4I, lane M/S) and a smear composed of a family of Y structures with a variable branchpoint due to the range of insertion sites in the target DNA (bracket in Figure 4I, lane S). Digestion with *Pst*I would also be expected to generate a family of Y structures, but of higher molecular weight than those generated by *Sma*I. Each of these species could be detected with the appropriate digestion (Figure 4I, lanes S and P). These results are therefore consistent with the identification of species III as a two-ended integration product and of species I and II as one-ended integration events with or without cleavage of other end.

Although the nature of the group β and group γ species was not examined in detail, the data available provide some clues to their identity. Their relatively low mobility suggests that they are intermolecular integration products. Since the appearance of the γ group requires both OrfA and plasmid target, these species might result from insertion into multimeric copies of the target plasmid present in the preparation or from multiple insertions of the transposon into other transposon copies or into monomeric target plasmid molecules. At least some of the β group of bands are likely to represent autointegration events since they are generated in the absence of plasmid target DNA.

Effect of reaction conditions and terminal mutations in IRL and IRR on species I–III. The effect of different conditions on the relative yield of species I, II and III was examined. Figure 5A shows the effect of the divalent metal cations Mg^{2+} and Mn^{2+} and of DMSO on the reaction with the WT transposase preparation. With Mg^{2+} alone (lane 2), species III was approximately twice as abundant as II. Addition of DMSO (lane 1) stimulated the production of all three species. Replacement of Mg^{2+} by Mn^{2+} (lane 3) stimulated production of all three species but had a stronger effect on the production of species I and II, resulting in approximately equal intensities for all three bands.

The results presented in Figure 5B confirm that OrfAB alone in the presence of Mg^{2+} (lane 3) exhibits very weak activity. On addition of DMSO (lane 1) or in the presence of Mn^{2+} (lane 5), some enhancement in activity was detected resulting principally in an increase in the one-end transfer species I and II. Premixed OrfAB+OrfA preparations (lanes 2, 4 and 6) gave results similar to those obtained with WT protein preparations.

Results obtained with an IRL^-/IRR^+ mutant substrate supported the interpretation that species I and II are the result of one-end transfer (Figure 5C). As for the wild-type circle junction (Figure 5B), little activity was observed with OrfAB alone in the presence of Mg^{2+} (lane 3), Mg^{2+} and DMSO (lane 1) or Mn^{2+} (lane 5), while addition of premixed OrfAB+OrfA resulted in increased activity (lanes 2, 4 and 6). However, in contrast to the wild-type junction, for which an increase in the amounts of all three species occurred under these conditions, the mutant

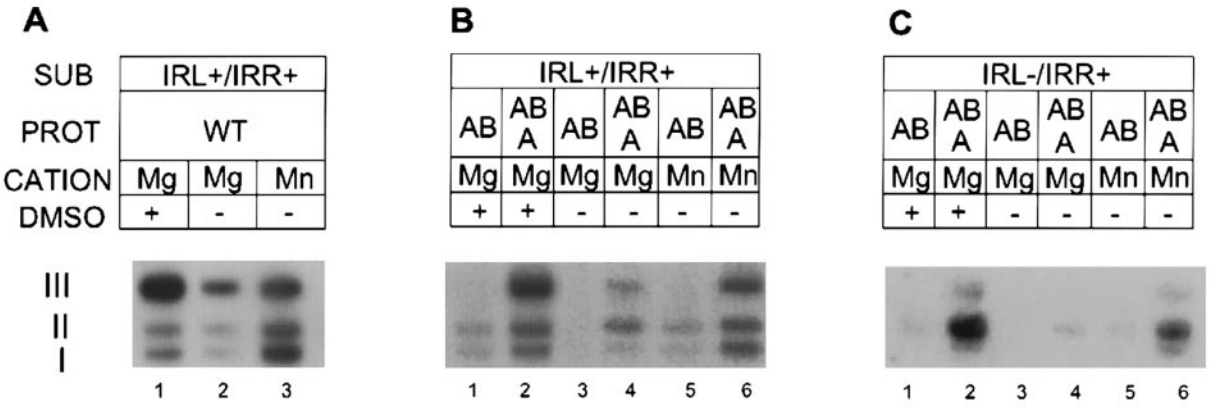

Fig. 5. Effect of Mn^{2+}, DMSO and terminal dinucleotide 5′-CA-3′ on I–III. Symbols and hybridization are as described for Figures 3 and 4. The tables above each panel show the components of each reaction. 'SUB' indicates the type of transposon circle used as substrate, IRL^+/IRR^+ and IRL^-/IRR^+ as in Table 1; 'PROT' indicates the protein preparation used: WT (0.9 μg); AB, OrfAB (0.48 μg); A, OrfA (0.54 μg); 'CATION' indicates the type of divalent cations: Mg, magnesium; Mn, manganese. Reactions contained 10% DMSO where indicated.

junction generated mostly species II resulting from one-ended cleavage and transfer. A similar pattern was obtained with the mutant IRR (data not shown). The presence of DMSO (Figure 5C, compare lanes 2 and 4) or Mn^{2+} (compare lanes 4 and 6) resulted in a strong stimulation of all three species.

Intramolecular products. All species which migrate faster than the open circular form of the transposon circle (α in Figure 3) are presumably products of intramolecular transposition as observed *in vivo* (Ton-Hoang *et al.*, 1997). As in intermolecular transposition, potential intramolecular products involving both transposon ends and single ends might also be expected to arise (Figure 6A, species b and c, d–k and h–k, respectively).

To analyse these products further, reactions were carried out with the WT protein preparation in the absence of target plasmid DNA and first separated in a 0.7% gel (as shown in Figure 3). The α group of species were cut from the gel and either introduced directly into a 1% agarose gel or incubated with *Msc*I (an enzyme which cleaves within IRL and IRR) or *Sma*I (which has a single recognition site in the middle of the transposon). The various species were revealed by Southern hybridization using a transposon-specific oligonucleotide probe (Figure 6B).

(i) Two-ended intramolecular products. The most prominent feature of the gels is a diagonal composed of relatively well defined species (D), which is similar in both the undigested and digested samples (Figure 6B, panels a–c). These may represent unknotted adjacent deletions expected to migrate as open circular molecules in the non-digested sample, linear molecules in the *Msc*I-digested sample (Figure 6B, panel b), and either linear or open circular forms in the *Sma*I-digested sample (Figure 6B, panel c) (depending on whether the deletion event removed the unique *Sma*I site) (Figure 6A, species c). The non-random distribution is presumably the result of target site preferences in the deletion reaction. Thus, as was observed *in vivo* (Ton-Hoang *et al.*, 1997), the *in vitro* reaction generated a significant proportion of adjacent deletions. Inversion products do not appear as a major product of the reaction (but see below). Such species should migrate at the level of open circular transposon circles in the undigested sample and as a vertical group of spots or smear in the *Msc*I-digested sample (Figure 6B, panel b). No significant material of this type was detected.

Besides these major products, an arc of regularly spaced spots (K) is clearly visible in the undigested sample (Figure 6B, panel a). The species composing this arc behave as expected for catenated and knotted molecules. The arc disappeared following digestion with *Msc*I. Digestion with *Sma*I (but not *Msc*I) resulted in a series of spots, K′, which migrated at the level of linear transposon DNA and occupied positions equivalent to alternative members of the K group. This is the behaviour expected of knotted inversion circles (Figure 6A, species e). Each spot should contain a family of molecules with the same topological complexity (a defined odd number of nodes) but in which the target position can vary. Digestion with *Sma*I would produce molecules having the size of the linear transposon. Digestion with *Msc*I, which cleaves within each transposon end, should produce fragments of variable size within the family and these would not appear as a defined species. Similarly, those alternative members of the K group which disappear on digestion with either enzyme may represent equivalent families of catenated deletion products with even numbers of nodes (Figure 6A, species f and g). Although the overall mass is identical, since the target position can vary, the relative size of the two catenated circles will vary and cleavage will produce fragments of variable size.

(ii) One-ended products. Some of the minor products might correspond to one-ended events predicted in Figure 6A, species h–k. In addition to species L, C and O, which migrated at the position expected for the linear transposon following *Msc*I (Figure 6B, panel b) or *Sma*I (Figure 6B, panel c) digestion, *Msc*I digestion generated a horizontal smear (S) which migrated with linear transposon DNA in the second dimension. This could correspond to species h–k (Figure 6A) since digestion by *Msc*I would be expected to generate molecules which are essentially linear transposon derivatives. On the other hand, digestion of h and k with *Sma*I would generate a family of α molecules and of Y forms respectively, which would be expected to migrate more slowly than linear transposon derivatives in the second dimension. The vertical spot, Z, generated by *Sma*I (Figure 6B, panel c) may represent some of this

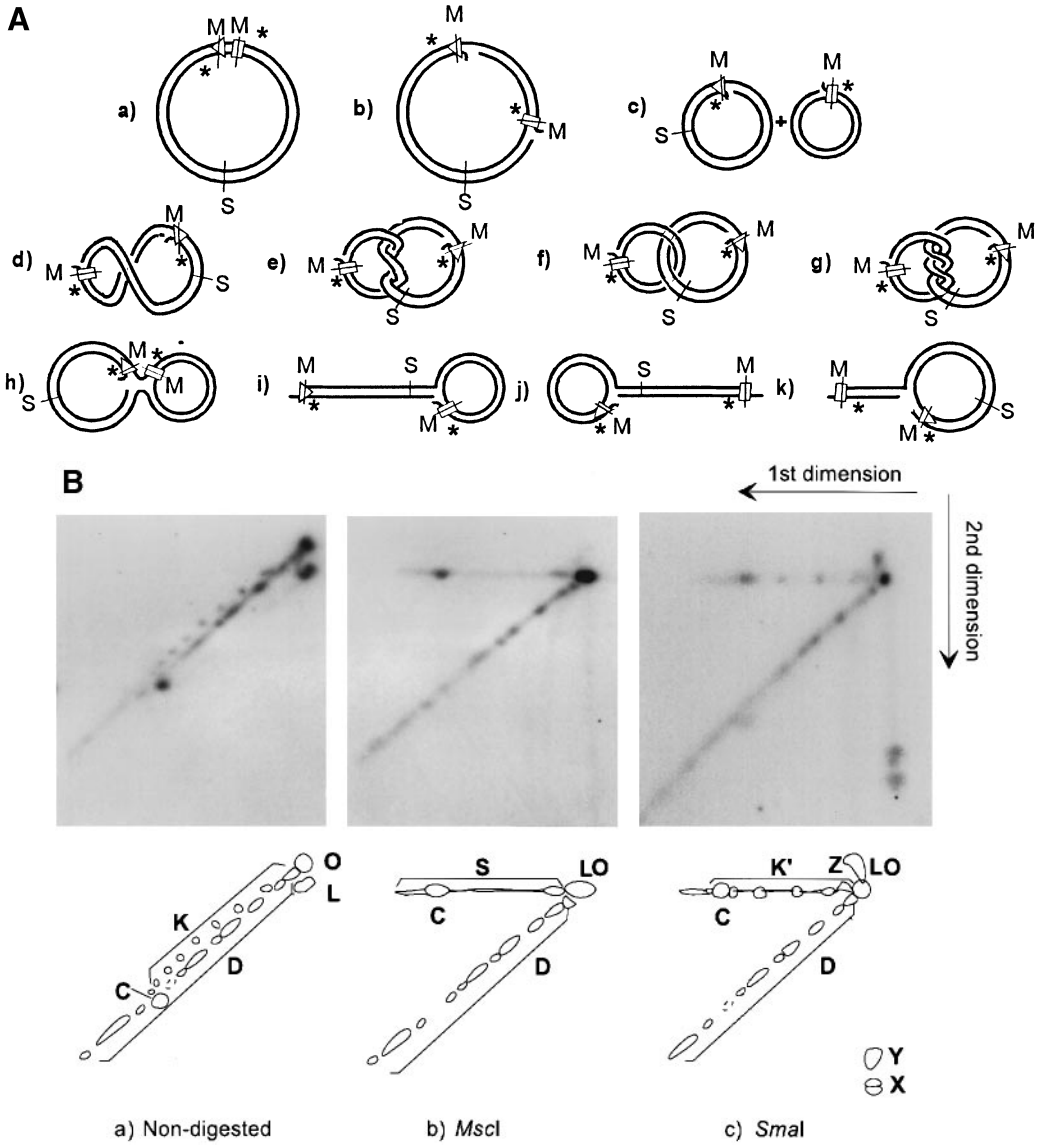

Fig. 6. Intramolecular transposition products. (**A**) Predicted structures for adjacent deletions (c), inversions (b), the topological series of knotted inversion (d and e) and catenated deletions (f and g) and one-ended integration products (h–k). (a) shows the unrearranged transposon circle substrate. Symbols are as described in Figures 3 and 4. M and S represent cleavage sites for *Msc*I and *Sma*I respectively. (**B**) Analysis of intramolecular transposition products α by two-dimensional agarose gel electrophoresis (0.7% in the first dimension and 1% in the second dimension in TAE buffer) and Southern blotting with B21 as a probe. The DNA preparations were undigested in the first dimension and undigested (a) or digested *in situ* with *Msc*I (b) or *Sma*I (c) in the second dimension. Below, drawings of the gels indicate the identities of different features. C, L and O represent closed circle, linear and open circle forms of the substrate respectively. The group of spots, D, represents adjacent deletions. In (a) they are gapped circles while in (b) digestion with *Msc*I gives rise to linearized derivatives and digestion with *Sma*I (c) results in a mixture of circles and linear forms depending on the retention of a *Sma*I site in the deleted product. An arc of knotted inversions and catenated deletions, K, is indicated in panel a. The knotted inversions are converted to linear forms, K', on digestion with *Sma*I (c). Forms S, X, Y and Z are described in the text.

type of product. Furthermore, the *Sma*I-digested sample exhibited two prominent spots (X and Y) at the bottom right-hand corner. These could correspond to the linear 'tail' and the branched circular component of i and j (Figure 6A), since target is located between the attacking end and the *Sma*I site in these species. Some of these interpretations were confirmed by analysis of the products obtained with a IRL^{-}/IRR^{+} substrate where a significant reduction of two-ended products D and K was observed (data not shown).

Although we have not undertaken an exhaustive analysis of the different intramolecular transposition products, it is clear from the results presented above that intramolecular transposition using the circle junction resulted in a majority of two-ended products compared with one ended insertions. Furthermore, the majority of the two-ended products were topologically simple deletions with a minor fraction of catenated deletions and knotted inversions.

Effect of substrate supercoiling

The experiments described so far have made use of a supercoiled donor molecule. To determine whether supercoiling of the donor is important for insertion, the activity of linear molecules carrying the circle junction was examined. The transposon donor molecules were *Pst*I–*Bam*HI fragments of approximately 1 kb generated from plasmids pMiT130, pBST2 and pBST3. These plasmids carry respectively: the wild-type circle junction

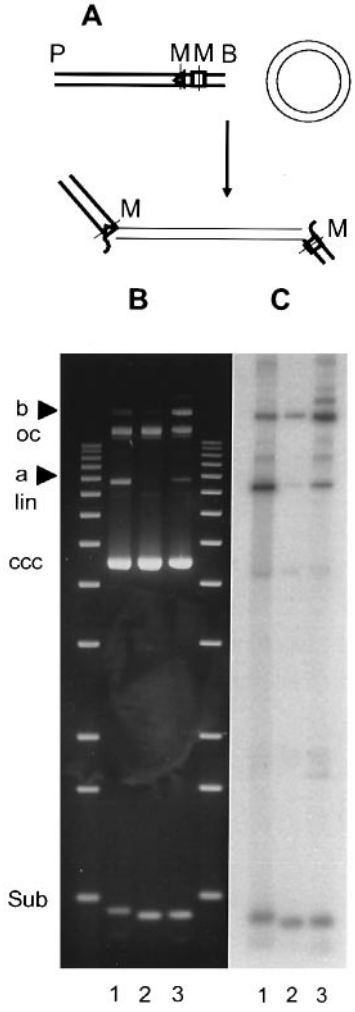

Fig. 7. Integration with linear junction substrate. (**A**) Consequences of two-ended integration of a linear molecule carrying the circle junction into a circular plasmid target. The symbols are identical to those in Figure 4. P, B and M indicate *Pst*I, *Bam*HI and *Msc*I restriction sites respectively. (**B**) Ethidium bromide-stained agarose gel (1.2%) of integration products with linear substrates, the WT protein preparation and plasmid pAPT110 as target. The flanking lanes show molecular mass standards (1 kb ladder). The various DNA species are indicated: 'ccc', 'lin' and 'oc' represent covalently closed circular, linear and open circular forms of target plasmid pAPT110 respectively. The two-ended integration product (a), and a probable one-ended integration product (b) are discussed in the text. Reactions in lanes 1–3 were carried out with *Pst*I–*Bam*HI fragments of pMiT130, pBST2 and pBST3, carrying IRL^+/IRR^+, IRL^-/IRR^-, IRL^-/IRR^+ junction respectively. (**C**) Southern hybridization of the gel shown in (A) using oligonucleotide O17 as a probe.

(IRL^+/IRR^+); a circle junction with an inactivated IRL (IRL^-/IRR^+); and a circle junction with both ends inactivated (IRL^-/IRR^-) (Ton-Hoang *et al.*, 1997). The target molecule was a supercoiled p15A-based plasmid, pAPT110 (~7 kb; Polard and Chandler, 1995). Reactions were carried out using a WT protein preparation. Two-ended integration of both transposon ends into a circular target molecule is expected to generate a linear molecule in which the target is flanked by both halves of the transposon donor (Figure 7A). The reaction with the wild-type junction generated a prominent band, 'a' (Figure 7B, lane 1), with the size expected (~8 kb) for a linear molecule composed of both target and donor DNA. This band was not visible with a donor fragment containing IRL^-/IRR^- (Figure 7B, lane 2) and was significantly weaker with the IRL^-/IRR^+ donor (Figure 7B, lane 3) suggesting that it is the product of two-ended integration.

An additional species, 'b', which migrated above the open circular form of the target plasmid, appeared more prominent with the single end mutant (lane 3). Hybridization of the gel with a probe specific for IRR (Figure 7C) confirmed that both 'a' and 'b' exhibited homology with the transposon donor and revealed several additional high molecular weight bands, particularly with the IRL^-/IRR^+ donor fragment (lane 3). The IRL^-/IRL^- donor (lane 2) generated a faint band corresponding to 'b' and a signal for 'a' which was hardly detectable. The nature of 'b' and the other species with homology to the transposon was not examined further but it seems probable that they arose from one-ended transfer events.

The nature of species 'a' was confirmed by digestion with *Msc*I which cleaves in both transposon terminal IRs but not within the target plasmid. Digestion should remove the flanking transposon DNA and generate a fragment with the size of linear target (7 kb) (data not shown).

Supercoiling of the donor molecule is therefore not necessary for integration. The results also confirm those obtained with a supercoiled transposon circle indicating that mutation of the ends compromises strand cleavage and/or strand transfer.

Effect of spacing between the transposon ends

In the circle junctions used here, the abutted IRL and IRR sequences are 3 bp apart. To determine the degree to which this natural spacing is necessary for efficient integration, a series of plasmids was constructed in which the spacing was varied between 2 bp and 13 bp and the relevant 1 kb *Pst*I–*Bam*HI fragments were used as linear transposon donors in a standard reaction with pAPT110 as the target molecule. The results are shown in Figure 8. Separation of two ends from 3 bp up to 9 bp or by one helical turn (13 bp) significantly diminished the efficiency of two-ended integration (compare Figure 8A and B, lanes 2, 4 and 5). Changing the spacer from 3 bp to 2 or 4 bp seemed also to affect the pattern of integration. As shown in Figure 8A, lanes 1–3, the junction with wild-type spacing (3 bp) gave a maximal level of the two-ended integration product 'a' whereas a junction with 2 or 4 bp spacing yielded a higher proportion of one-ended integration products 'b'. The percentage of species 'a' as a function of total intermolecular integration products is presented in Figure 8C. These data demonstrate that a spacing of 3 bp found at the natural IS*911* circle junction is optimal for integration.

Discussion

We describe here an *in vitro* system in which a purified IS*911*-based transposon circle substrate is efficiently integrated into a target DNA molecule. The reaction required IS*911*-encoded proteins and, like other *in vitro* transposition reactions, a simple buffer with a divalent cation but no external energy source [see Mizuuchi (1992b) for review]. We have identified several intermolecular reaction products which include simple insertions, in which the two transposon ends have undergone integration into the

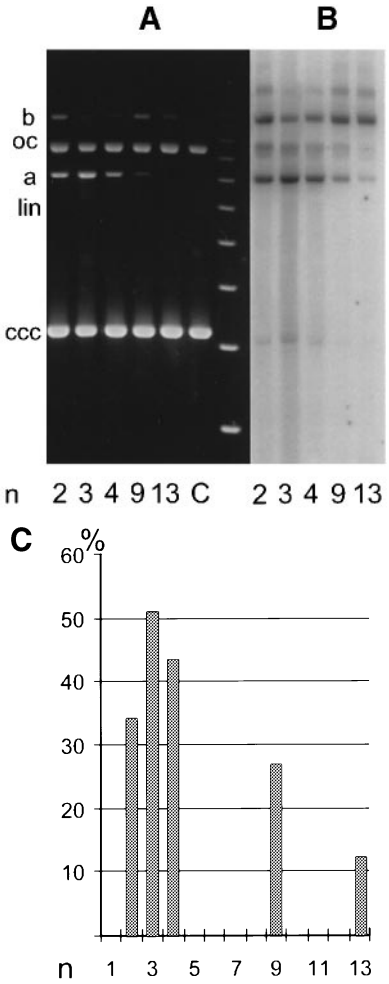

Fig. 8. Spacing effect of ends at circle junction. (**A**) Ethidium bromide-stained 0.7% agarose gel of an integration reaction with linear substrates, the WT protein preparation and pAPT110 as target. Reaction conditions were identical to those used in Figure 7. Substrates were *Pst*I–*BamH*I fragments of: lane 1, pBST10 (2 bp spacer); lane 2, pMiT130 (3 bp spacer); lane 3, pBST11 (4 bp spacer); lane 4, pBST13 (9 bp spacer); lane 5, pBST12 (13 bp spacer); lane 6, control plasmid pZBT18 (Zerbib *et al.*, 1990a). The position of substrate DNA, which migrates rapidly in this gel, is not shown. (**B**) Southern hybridization of the gel shown in (A) using the transposon-specific O17 oligonucleotide as a probe. (**C**) Results of phosphorimager quantification. Percentage of two-ended integration product as a function of total intermolecular transposition products.

target site, and several species in which only one end of the transposon has undergone strand transfer. The reaction also generated various intramolecular transposition products, essentially adjacent deletions. These results provide further support for the idea that circles can act as intermediates in IS*911* transposition.

Role of OrfA in transposition

An important observation in this study was that, in addition to the transposase, OrfAB, a second IS*911* protein, OrfA, is clearly required for efficient intermolecular integration. OrfA essentially represents the amino-terminal domain of OrfAB. The major effect of OrfA is to stimulate two-ended strand transfer, although one-ended integration was also somewhat enhanced. Although the results should be interpreted with caution, since the specific activity of our protein preparations has not been determined, the optimal efficiency of the intermolecular integration appeared to occur at a molar OrfA/OrfAB ratio of 4–6. This is close to that estimated to be produced by natural protein expression of IS*911* (Polard *et al.*, 1991).

In the case of other insertion sequences, it is generally believed that the transposase alone mediates all cleavage and strand-transfer steps necessary for mobility. Indeed, this has been shown to be the case for the prokaryotic ISs, IS*10* and IS*50*, and for eukaryotic elements of the mariner/Tc family (see Kleckner *et al.*, 1996; Plasterk, 1996; I.Goryshin and W.Reznikoff, personal communication). It is also true for retroviruses [see Andrake and Skalka (1996) for review]. Where second IS-encoded proteins are involved, these generally represent subdomains of the transposase and act as negative regulators of transposition activity, either by competing with transposase for binding to the ends (e.g. InsA of IS*1*; Zerbib *et al.*, 1990a,b) or by forming inactive heteromultimers (e.g. Inh of IS*5* ; de la Cruz *et al.*, 1993). Stimulation of transposition as described here has not previously been described.

In the case of the more complex transposons, bacteriophage Mu and Tn*7*, a second protein (MuB and TnsC respectively) cooperates with the transposase (MuA and TnsA/B respectively) to stimulate transposition. These proteins are produced from genes distinct from the corresponding transposase. Both MuB and TnsC share an ATP-utilizing capacity which can modulate their activity. They are both involved in trapping target DNA and distinguishing (and avoiding) DNA already carrying the ends of the cognate element, a process known as transposition immunity. A potentially similar situation may occur in the case of insertion sequences of the IS*21* family. Here, two consecutive open reading frames are necessary for transposition. The product of the first, IstA, carries a DDE-like motif presumed to be part of the catalytic site of the enzyme (Haas *et al.*, 1996) and cleaves an IS*21* junction resembling the IS*911* circle junction (Reimmann and Haas, 1990) whereas the product of the second, IstB, has a potential ATP-binding site (Haas *et al*., 1996). IstB may be equivalent to MuB and TnsC.

Although the requirement for two proteins for efficient IS*911* integration is reminiscent of the behaviour of Mu and Tn*7*, there appear to be several major differences between IS*911* and these transposons. OrfA is not produced from a distinct gene but is essentially the amino-terminal domain of the frameshifted OrfAB transposase; the stimulatory effect of OrfA does not require an energy source and the protein does not exhibit a typical ATP-binding motif. In addition, neither MuB and TnsC exhibit marked sequence-specific DNA binding activity whereas OrfA specifically recognizes the terminal IS*911* IRs (Polard, 1993; B.T.-H and L.Haren, unpublished observations).

OrfA may directly stimulate strand cleavage or transfer (cf. MuB and TnsC; Surette and Chaconas, 1991; Surette *et al.*, 1991; Bainton *et al.*, 1993), participate in synapsis by coordinating events at both ends, or simply enhance target acquisition. The observation that preincubation of OrfA and OrfAB increases the efficiency of the integration reaction suggests that the effect of OrfA is transmitted by direct interactions between the two proteins. In this light it should be noted that, OrfAB and OrfA not only share a common potential helix–turn–helix (HTH) domain but also a leucine-zipper motif which, as a consequence of

the frameshift, differs only in the last heptad. An attractive hypothesis is that OrfA modulates the transposase activity by protein–protein interaction via this multimerization motif (L.Haren, P.Polard, C.Normand and M.Chandler, in preparation).

Cleavage and strand transfer at the circle junction

One result of the creation of the circle junction is that it brings both transposon ends into proximity in a configuration which is likely to enhance transposition efficiency. Several transposable elements, including IS*2* (Szeverenyi *et al.*, 1996), IS*3* (Spielmann-Ryser *et al.*, 1991), IS*21* (Reimmann *et al.*, 1989) and IS*30* (Olasz *et al.*, 1993), have been shown to undergo highly efficient transposition when two terminal inverted repeats are brought together in this way. In the case of IS*911* this can be understood in terms of OrfAB-mediated single strand cleavage at each tip of the element in the junction to uncover a 3′-OH and transfer of both ends into a suitable target. The results suggest that, as with several other transposons such as Tn*7* (Bainton *et al.*, 1991; Gary *et al.*, 1996), Tn*10* (Haniford and Kleckner, 1994), Tc*1* (Vos and Plasterk, 1994), retroviruses (Bushman and Craigie, 1991), the events at each end are not necessarily concerted. Single end cleavages on IS*911* transposon circles in the presence of OrfAB alone are readily observed *in vivo* and result in the appearance of open circular species. Mapping of the cleavage site on such molecules showed specific nicks at either one or the other end (unpublished results). Moreover, the use of a single end mutant in these *in vitro* studies resulted in an increase in the proportion of open circular molecules indicating that the mutant end must be cleaved inefficiently and that this does not greatly affect cleavage of the wild-type end at the junction (B.Ton-Hoang, P.Polard, L.Haren and M.Chandler, in preparation). This non-concerted behaviour is further illustrated by the relatively high levels of single-end insertion products observed in these experiments.

What are the steps which lead to direct insertion using the abutted ends in the circle junction? Several different and non-exclusive pathways could operate. The simplest would be passage by two coordinated single-strand breaks at each end, equivalent to a double-strand break effectively linearizing the transposon, followed by strand transfer at both cleaved ends. Preliminary data from kinetic studies suggest that linearization of transposon circles may indeed precede their insertion. Alternatively, integration could occur in a stepwise process by consecutive cleavage and transfer of each end. It is also possible that transfer of both ends is simply aided by their proximity. Whatever the pathway, the maximal two-ended transfer efficiency observed with 3 bp spacer suggests some coordination of events at the natural circle junction. Further investigation of the kinetics of formation of the different intermolecular species will be required in order to clarify the exact pathway used.

Reaction conditions

Changes in the reaction conditions can have profound effects on the relative proportion of the different products. In reactions using an IRL^+/IRR^+ circle junction, a high proportion of simple insertions (species III) was observed in the presence of the divalent cation Mg^{2+}. Substitution for Mn^{2+} resulted in a stimulation of the overall reaction but the effect was more pronounced with the one-ended integration species I and II. These results are consistent with those obtained in OrfAB-mediated figure-of-eight formation *in vitro* (Polard *et al.*, 1996) where substitution of Mg^{2+} by Mn^{2+} not only enhanced the activity observed with wild-type IS*911* ends but stimulated the activity of a substrate mutated at both ends which is normally inactive *in vivo*. This reduction in stringency is typical of several transposition and recombination systems (Katzman *et al.*, 1989; Drelich *et al.*, 1992; Copeland *et al.*, 1993; van Gent *et al.*, 1996).

These effects are also observed in experiments with IRL^-/IRR^+ junctions. In the biological assay using Mg^{2+}, simple insertions occurred with a frequency ~50-fold lower than with the wild-type junction (data not shown) whereas in the presence of DMSO the frequency was less than 10-fold lower. Thus, reaction conditions can influence the efficiency of rescue of a single defective end in the circle junction. In the physical assay however, in contrast to the IRL^+/IRR^+ junction, Mn^{2+} and DMSO were found to stimulate formation principally of species II. While the exact mechanism is not clear, DMSO is known to relax some reaction requirements for assembly of an active Mu transpososome (Craigie and Mizuuchi, 1986; Mizuuchi and Mizuuchi, 1989; Baker and Mizuuchi, 1992).

Intramolecular transposition: inversion and deletions

Two-dimensional gel electrophoresis indicated that both deletions and inversions were generated in an intramolecular reaction. As was also observed *in vivo* (Ton-Hoang *et al.*, 1997), the *in vitro* system generated a majority of adjacent deletions relative to inversions. A similarly strong bias towards deletions has also been observed in the case of IS*903* and IS*1* although the exact transposition mechanism which generates these products may not be the same (Weinert *et al.*, 1983; Turlan and Chandler, 1995). In contrast, for IS*10*, the major intramolecular products were inversions (see Kleckner *et al.*, 1996; Benjamin and Kleckner, 1992; Chalmers and Kleckner, 1996) while in the case of γδ, both types of product were observed (Wang *et al.*, 1994).

Two-dimensional gel analysis also provided information concerning the way in which transposon ends may find their target site. Catenated deletions represent products in which supercoils are trapped within the recombining molecules and can be explained by random collision of the transposon ends with target sequences. The vast majority of deletion products, however, were uncatenated. This implies that supercoils are actively excluded in the majority of events, an observation consistent with a tracking mechanism for target site location. The knotted inversion circles and catenated deletions may simply reflect molecules in which this processive behaviour had failed. Similar observations have been made in the Cre-*loxP* site-specific recombination system with mutant Cre recombinases or altered *loxP* sites (Abremski *et al.*, 1988).

Taken together with the results obtained from *in vivo* experiments (Ton-Hoang *et al.*, 1997), these results demonstrate that transposon circles are efficient transposition donors, consistent with the idea that they represent an intermediate form in the transposition of IS*911*. They also

demonstrate that OrfA is required for intermolecular transposition. Since OrfA shares two functional domains with OrfAB, those for DNA-binding and for multimerization (L.Haren, P.Polard, C.Normand and M.Chandler, in preparation) but not the transposase catalytic site, it will be important in future studies to determine the exact role of OrfA in IS*911* transposition. It will also be important to determine the sequence of cleavages and strand-transfer events leading to integration of the transposon circle.

Materials and methods

Bacterial strains and media

The bacterial strain used in the preparation of cell extracts was Mi898, a derivative of MC1061 (*ara*D139, Δ[*ara leu*], *gal*U, *gal*K, *hsd*M, *hsd*S, *rps*L Δ[*lacIOPZYA*]X74) carrying a deletion of the endonuclease I gene *end*A (Polard *et al.*, 1996). Supercoiled transposon circles were generated in JS219 (*srl*C::Tn*10*, *rec*A1, *mal*Pp::*lacI*^{Q}, *ara*D139, Δ[*ara leu*], *gal*U *gal*K, *hsd*M, *hsd*S, *rpls*L Δ[*lacIOPZYA*]X74) as host (Polard *et al.*, 1992).

Cultures were grown in Terrific Broth (Sambrook *et al.*, 1989) supplemented with ampicillin (100 μg/ml) and kanamycin (25 μg/ml). Selection of Cm^{R} transformants was carried out on L plates containing 30 μg/ml chloramphenicol.

Plasmids

The construction of pAPT99 was described previously (Polard *et al.*, 1992). The equivalent plasmids carrying mutations of terminal dinucleotides 5′-CA-3′ in IRL (pAPT177), IRR (pAPT178) were constructed by replacing an *Msc*I fragment, carrying an *orf*A–*lac*Z fusion from pAPT180 and pAPT181 by an *Msc*I fragment, carrying a Cm^{R} cassette from pAPT99. Plasmid pAPT111 in which OrfAB is placed under the control of the p_{lacUV5} promoter has also been described (Polard and Chandler, 1995b).

The transposase expression plasmid, pAPT158 (8208 bp) is identical to pAPT111 except for the ribosome-binding site located between the p_{lacUV5} promoter and the OrfAB initiation codon. The natural IS*911* ribosome-binding site carried on an *Xba*I–*Bam*HI fragment in pAPT111 was substituted for a similar restriction fragment carrying the bacteriophage T7 ϕ10 ribosome-binding site sequence from pAR30-39 (Studier and Moffatt, 1986).

The OrfA, OrfB and WT expression plasmids pAPT156 (7313 bp), pAPT157 (7959 bp) and pAPT155 (8207 bp) were assembled in the same way as the transposase expression plasmid pAPT158, using plasmids pAPT151, pAPT152 and pAPT150 respectively (Polard *et al.*, 1992).

Plasmids pBST2 and pMiT130 have been described previously (Ton-Hoang *et al.*, 1997). Plasmid pBST3 with mutant IRL at the junction was constructed in a similar way to pBST2.

Plasmid pBST10 (2 bp spacer) was constructed in two steps. First, the resident *Nde*I site of pMiT130 was removed by *Nde*I digestion followed by treatment with a 'blunting kit'(Amersham) and religation. The *Bal*I fragment of this plasmid was then replaced by two complementary oligonucleotides with an *Nde*I site: 5′-CCAGTTTTTGTTGACCA-CTT**CATATG**AAGTGGCACACTGAATTTGG-3′ and 3′-GGTCAAA-AACAACTGGTGAA**GTATAC**TTCACCGTGTGACTTAAACC-5′.

Plasmid pBST11 (4 bp spacer) was derived from pBST10 by treatment of *Nde*I-digested plasmid with Klenow fragment. pBST12 (13 bp spacer) was constructed by insertion of two complementary oligonucleotides (carrying a *Kpn*I site) at the *Nde*I site of pBST10: 5′-TAG**GGTACC**GC-3′ and 3′-C**CCATGG**CGAT-5′. pBST13 (9 bp spacer) was obtained by treating *Kpn*I-digested pBST12 with the 'blunting kit'(Amersham) followed by ligation.

Plasmid pAPT110 used as a target for integration of linear substrate has been described previously (Polard and Chandler, 1995). pDAG92 is a ColE1-based replicon carrying the *lac*Z gene under control of promoter p_{ara}, a generous gift from D.Lane (the exact construction of this plasmid is available on request).

Preparation and purification of transposon circles and linear integration substrates

Strains carrying different combinations of the transposon-donor and transposase-donor were constructed by successive transformations of JS219. Transposon circles were extracted by the alkaline lysis method (Sambrook *et al.*, 1989) and gel purified using the Biotrap system (Schleicher & Schuell).

The linear integration substrates were prepared by digestion of different plasmids with *Bam*HI and *Pst*I, separation by electrophoresis on agarose gel and purification with GenElute spin columns (SUPELCO Inc.).

Purification of OrfAB, OrfA and WT proteins

A culture of MB898 carrying the OrfAB expression plasmid pAPT158, the OrfA (pAPT156) or the WT (pAPT155) expression plasmids and grown at 30°C overnight in Terrific Broth containing kanamycin was diluted into 500 ml of the same medium at an OD_{600} of 0.1. Protein expression was induced at an OD_{600} of 0.6 with isopropyl-β-D-thiogalactopyranoside (IPTG) to a final concentration of 1 mM. Growth was continued for an additional 90 min, then the cells were harvested by centrifugation and treated as described (Polard *et al.*, 1996). For the transposase, OrfAB, the 40% ammonium sulfate pellet was resuspended in 10 ml of buffer A [25 mM HEPES pH 7.5, 2 mM EDTA, 1 mM dithiothreitol (DTT), 20% glycerol] with 0.2 M KCl, centrifuged to remove any insoluble materials and loaded on to a 5 ml Hitrap heparin–Sepharose column (Pharmacia Inc.). The column was first extensively washed with the same buffer, then with buffer A (0.4 M KCl) and buffer A (0.7 M KCl). Bound transposase was eluted with 20 ml of buffer A (1 M KCl). The fractions were pooled and dialysed against buffer A (0.4 M KCl).

The same procedure was carried out for purification of OrfA, except that the 30% ammonium sulfate pellet was washed first in 10 ml of buffer A (0.1 M KCl), after centrifugation the supernatant was discarded and the pellet was solubilized in 4 ml of buffer A (1 M KCl and 10 mM CHAPS) for 3 h with gentle agitation at 4°C. The solubilized proteins were diluted with 2 vol. of buffer A (0 M KCl) and applied to a heparin–Sepharose column, equilibrated with buffer A (0.33 M KCl and 3.3 mM CHAPS). After a similar washing step with the same buffer and buffer A (0.6 M KCl and 2 mM CHAPS), OrfA was eluted with buffer A (1 M KCl, 2 mM CHAPS) and dialysed against buffer A (0.4 M KCl, 2 mM CHAPS).

The WT preparation was obtained in similar way, except that the 40% ammonium sulfate pellet was resuspended first in 5 ml of buffer A (0.2 M KCl). The solution was spun for 5 min in a microcentrifuge, the soluble material (fraction I) was kept on ice and the pellet was solubilized in buffer A (1 M KCl, 10 mM CHAPS) as for OrfA (fraction II). Fractions I and II were pooled, adjusted to 0.33 M KCl, 2 mM CHAPS and the purification was continued as for OrfA. Proteins were analysed by SDS–PAGE and Coomassie staining as described (Sambrook *et al.*, 1989) and their concentration was determined using a Bio-Rad Protein Assay with BSA as standard.

Samples were frozen as aliquots in liquid nitrogen and stored at –80°C until required. They were stable for at least several months.

Cell-free integration system

The standard reaction was performed in a final volume of 30 μl containing 600 ng DNA target (pDAG92) (0.12 pmol), 50 ng of transposon circles (0.02 pmol), 18 μl of the different protein preparations (in dilution buffer A, 0.4 M KCl) in 25 mM HEPES (pH 7,5), 0.3 M KCl, 10 mM $MgCl_2$, 2 mM DTT, 20 ng/ml BSA, 10% DMSO and 14% glycerol. Where indicated, $MgCl_2$ was replaced by $MnCl_2$ without DMSO. Standard reactions were carried out at 30°C for 3 h. Reactions were terminated and deproteinized by adding 30 μl of 25 mM EDTA, 0.6 mg/ml Proteinase K, 2% SDS, incubated for 1 h at 37°C and treated with a mixture of phenol/chloroform (1:1) followed by extraction with chloroform and ethanol precipitation.

The integration reaction with linear substrates were performed under standard conditions with 900 ng of WT preparation, except that pAPT110 was used instead of pDAG92 as target.

DNA procedures

Standard techniques were used for DNA manipulation and cloning (Sambrook *et al.*, 1989). Restriction and DNA modifying enzymes were purchased from Biolabs. DNA fragments were isolated using Geneclean (Bio101).

Southern blots were probed with oligonucleotides O17 (which hybridizes within the IRR sequence), B21 (which hybridizes within the transposon between 186 and 211 bp from IRL and IRR) or B7 (which hybridizes within the target plasmid pDAG92) as indicated. They have the following nucleotide sequences. O17: 5′-CCAGTTTTTGTTG-ACCCACTT-3′; B21: 5′-GGATGACCTTTTGAATGACCTTTTAA-3′; B7: 5′-CATGTTTGACAGCTTATCATCGATAA-3′.

Radiolabelling was with 8 pmol of oligonucleotides, 16 pmol of

[γ-^{32}P]ATP (5000 Ci/mmol, Amersham Inc.) and 1 unit of T4 kinase (NEB Inc.) in T4 kinase buffer (70 mM Tris–HCl pH 7.6, 10 mM $MgCl_2$, 5 mM DTT) for 1 h at 37°C. Labelled oligonucleotides were purified by filtration through Sephadex G25.

Gel electrophoresis and DNA quantification by hybridization

Reaction products were separated on 0.7% agarose gels in TAE buffer at 2.4 V/cm for 18 h (16 h for linear substrates) at room temperature. For two-dimensional electrophoresis analysis, the first dimension was in 0.7% Seakem Gold agarose (FMC), a 4 mm×8 cm gel strip containing intramolecular transposition species α was cut from the gel and divided longitudinally in two. One strip was kept at 4°C without further treatment, while the other was equilibrated in NeB 4 buffer (New England Biolabs) for 3 h at 4°C with agitation and buffer changes. The digestion was effected in a volume of 15 ml for 10 h with gentle agitation. After incubation was completed, strips were washed and equilibrated briefly with TAE and loading buffer. The second dimension was carried out in 1% agarose gel (Appligene) at 2.4 V/cm for 16 h at room temperature.

DNA hybridization was accomplished directly in the gel. The gel was dried for 70 min at 60°C, the DNA was denatured (0.5 M NaOH, 0.15 M NaCl, 20 min), and the gel neutralized in 0.5 M Tris (pH 8), 0.15 M NaCl. After a prehybridization step in 6× SSC, 0.5% SDS, 100 mg/ml calf thymus DNA and 0.1% non-fat milk for 6–8 h. Hybridization was carried out with a large excess of labelled oligonucleotide for 12–15 h in the same buffer. Both steps were performed at 8°C below the T_m of the oligonucleotide probe. The gel was then washed three times in 6× SSC, 0.1% SDS at room temperature, dried quickly and exposed either for autoradiography using Kodak XR5 film or, for quantification, in a Fuji X BAS1000 phosphorimaging system coupled to the PCBas software package.

Acknowledgements

We would like to thank all members of the Mobile Genetic Elements group (R.Alazard, G.Duval-Valentin, L.Haren, C.Normand, C.Turlan) and A.Hamiche for discussions and advice during the course of this work. We would also like to acknowledge A.J.Carpousis and D.Lane for critically reading the manuscript, B.Cointin for technical assistance and D.Villa for image processing. This work has benefited from grants from the CNRS (UPR9007), the 'Association pour la Recherche contre le Cancer' (6406), the 'Ligue Nationale contre le Cancer' (leg Petijean), the 'Association National de Recherche Contre le SIDA', Région Midi-Pyrenées and an EU network grant in the HCM programme. B.T.-H was partially supported by a grant from the 'Fondation pour la Recherche Medicale'.

References

Abremski,K., Frommer,B., Wierzbicki,A. and Hoess,R.H. (1988) Properties of a mutant Cre protein that alters the topological linkage of recombination products. *J. Mol. Biol.*, **202**, 59–66.

Andrake,M.D. and Skalka,A.M. (1996) Retroviral integrase, putting the pieces together. *J. Biol. Chem.*, **271**, 19633–19636.

Bainton,R., Gamas,P. and Craig,N.L. (1991) Tn*7* transposition *in vitro* proceeds through an excised transposon intermediate generated by staggered breaks in DNA. *Cell*, **65**, 805–816.

Bainton,R.J., Kubo,K.M., Feng,J.N. and Craig,N.L. (1993) Tn*7* transposition: target DNA recognition is mediated by multiple Tn*7*-encoded proteins in a purified *in vitro* system. *Cell*, **72**, 931–943.

Baker,T.A. and Mizuuchi,K. (1992) DNA-promoted assembly of the active tetramer of the Mu transposase. *Genes Dev.*, **6**, 2221–2232

Benjamin,H.W. and Kleckner,N. (1992) Excision of Tn*10* from the donor site during transposition occurs by flush double-strand cleavages at the transposon termini. *Proc. Natl Acad. Sci. USA*, **89**, 4648–4652.

Bushman,F.D. and Craigie,R. (1991) Activities of human immunodeficiency virus (HIV) integration protein *in vitro*: specific cleavage and integration of HIV DNA. *Proc. Natl Acad. Sci. USA* **88**, 1339–1343.

Chalmers,R.M. and Kleckner,N. (1996) IS*10*/Tn*10* transposition efficiently accommodates diverse transposon end configurations. *EMBO J.*, **15**, 5112–5122.

Chandler,M. and Fayet,O. (1993) Translational frameshifting in the control of transposition in bacteria. *Mol. Microbiol.*, **7**, 497–503.

Copeland,W.C, Lam,N.K and Wang,T.S. (1993) Fidelity studies of the human DNA polymerase alpha. The most conserved region among alpha-like DNA polymerase is responsible for metal-induced infidelity in DNA synthesis. *J. Biol. Chem.*, **268**, 11041–11049.

Craig,N.L. (1996) Transposon Tn7. *Curr. Top. Microbiol. Immunol.*, **204**, 27–48.

Craigie,R. and Mizuuchi,K. (1986) Role of DNA topology in Mu transposition: mechanism of sensing the relative orientation of two DNA segments. *Cell*, **45**, 793–800.

de la Cruz,N.B., Weinreich,M.D., Wiegand,T.W., Krebs,M.P. and Reznikoff,W.S. (1993) Characterization of the Tn5 transposase and inhibitor proteins: a model for the inhibition of transposition. *J. Bacteriol.*, **175**, 6932–6938.

Drelich,M., Wilhelm,R. and Mous,J. (1992) Identification of amino acid residues critical for endonuclease and integration activities of HIV-1 IN protein *in vitro*. *Virology*, **188**, 459–468.

Gary,P.A., Biery,M.C., Bainton,R.J. and Craig,N.L. (1996) Multiple DNA processing reactions underlie Tn*7* transposition. *J. Mol. Biol.*, **257**, 301–316.

Haas,D., Berger,B., Schmid,S., Seitz,T. and Reimmann,C. (1996) In Nakazawa,T. (ed.), *Molecular Biology of Pseudomonads*. ASM Press, Washington DC, pp 238–249.

Haniford,D. and Kleckner,N. (1994) Tn*10* transposition *in vivo*: temporal separation of cleavages at the two transposon ends and roles of terminal basepairs subsequent to interaction of ends. *EMBO J.*, **13**, 3401–3411.

Katzman,M., Katz,R.A., Skalka,A.M. and Leis,J. (1989) The avian retroviral integration protein cleaves the terminal sequences of linear viral DNA at the *in vivo* sites of integration. *J. Virol.*, **63**, 5319–5327.

Kleckner,N., Chalmers,R.M., Kwon,D., Sakai,J. and Bolland,S. (1996) In Saedler,H. and Gierl,A. (eds), *Transposable Elements*. Springer, Heidelberg, pp. 49–82.

Lewis,L.A. and Grindley,N.D. (1997) Two abundant intramolecular transposition products, resulting from reactions initiated at a single end, suggest that IS2 transposes by an unconventional pathway. *Mol. Microbiol.*, **25**, 517–529.

Mizuuchi,K. (1992a) Polynucleotidyl transfer reactions in transpositional DNA recombination. *J Biol. Chem.*, **267**, 21273–21276.

Mizuuchi,K. (1992b) Transpositional recombination: mechanistic insights from studies of Mu and other elements. *Annu. Rev. Biochem.*, **61**, 1011–1051.

Mizuuchi,M. and Mizuuchi,K. (1989) Efficient Mu transposition requires interaction of transposase with a DNA sequence at the Mu operator: implications for regulation. *Cell*, **58**, 399–408.

Olasz,F., Stalder,R. and Arber,W. (1993) Formation of the tandem repeat (IS30)2 and its role in IS30-mediated transpositional DNA rearrangements. *Mol. Gen. Genet.*, **239**, 177–187.

Plasterk,R.H. (1996) The Tc1/mariner transposon family. *Curr. Top. Microbiol. Immunol.*, **204**, 125–143.

Polard,P. (1993) Etude de l'elément transposable bacterien IS911: mise en evidence et charactérisation des facteurs necessaires a sa transposition. PhD thesis, Université Paul Sabatier, Toulouse.

Polard,P. and Chandler,M. (1995) An *in vivo* transposase-catalyzed single-stranded DNA circularization reaction. *Genes Dev.*, **9**, 2846–2858.

Polard,P., Prere,M.F., Chandler,M. and Fayet,O. (1991) Programmed translational frameshifting and initiation at an AUU codon in gene expression of bacterial insertion sequence IS911. *J. Mol. Biol.*, **222**, 465–477.

Polard,P., Prere,M.F., Fayet,O. and Chandler,M. (1992) Transposase-induced excision and circularization of the bacterial insertion sequence IS911. *EMBO J.*, **11**, 5079–5090.

Polard,P., Ton-Hoang,B., Haren,L., Betermier,M., Walczak,R. and Chandler,M. (1996) IS911-mediated transpositional recombination *in vitro*. *J. Mol. Biol.*, **264**, 68–81.

Prere,M.F., Chandler,M. and Fayet,O. (1990) Transposition in *Shigella dysenteriae*: isolation and analysis of IS911, a new member of the IS3 group of insertion sequences. *J. Bacteriol.*, **172**, 4090–4099.

Reimmann,C. and Haas,D. (1990) The *istA* gene of insertion sequence IS21 is essential for cleavage at the inner 3′ ends of tandemly repeated IS21 elements *in vitro*. *EMBO J.*, **9**, 4055–4063.

Reimmann,C., Moore,R., Little,S., Savioz,A., Willetts,N.S. and Haas,D. (1989) Genetic structure, function and regulation of the transposable element IS21. *Mol. Gen. Genet.*, **215**, 416–424.

Sambrook,J., Fritsch,E.F. and Maniatis,T. (1989) *Molecular Cloning: A Laboratory Manual*, 2nd edn. Cold Spring Harbor Laboratory Press, Cold Spring Harbor, NY.

Sekine,Y., Eisaki,N. and Ohtsubo,E. (1994) Translational control in production of transposase and in transposition of insertion sequence IS3. *J. Mol. Biol.*, **235**, 1406–1420.

Spielmann-Ryser,J., Moser,M., Kast,P. and Weber,H. (1991) Factors determining the frequency of plasmid cointegrate formation mediated by insertion sequence IS3 from *Escherichia coli*. *Mol. Gen. Genet.*, **226**, 441–448.

Studier,F.W. and Moffatt,B.A. (1986) Use of bacteriophage T7 RNA polymerase to direct selective high-level expression of cloned genes. *J. Mol. Biol.*, **189**, 113–130.

Surette,M.G. and Chaconas,G. (1991) Stimulation of the Mu DNA strand cleavage and intramolecular strand transfer reactions by the Mu B protein is independent of stable binding of the Mu B protein to DNA. *J. Biol. Chem.*, **266**, 17306–17313.

Surette,M.G., Harkness,T. and Chaconas,G. (1991) Stimulation of the Mu A protein-mediated strand cleavage reaction by the Mu B protein, and the requirement of DNA nicking for stable type 1 transpososome formation. *In vitro* transposition characteristics of mini-Mu plasmids carrying terminal base pair mutations. *J. Biol. Chem.*, **266**, 3118–3124.

Szeverenyi,I., Bodoky,T. and Olasz,F. (1996) Isolation, characterization and transposition of an (IS2)2 intermediate. *Mol. Gen. Genet.*, **251**, 281–289.

Ton-Hoang,B., Betermier,M., Polard,P. and Chandler,M. (1997) Assembly of a strong promoter following IS911 circularization and the role of circles in transposition. *EMBO J.*, **16**, 3357–3371.

Turlan,C. and Chandler,M. (1995) IS1-mediated intramolecular rearrangements: formation of excised transposon circles and replicative deletions. *EMBO J.*, **14**, 5410–5421.

van Gent,D.C., Ramsden,D.A. and Gellert,M. (1996) The RAG1 and RAG2 proteins establish the 12/23 rule in V(D)J recombination. *Cell*, **85**, 107–113.

Vos,J.C. and Plasterk,R.H. (1994) Tc1 transposase of *Caenorhabditis elegans* is an endonuclease with a bipartite DNA binding domain. *EMBO J.*, **13**, 6125–6132.

Wang,G., Xu,X., Chen,J.M., Berg,D.E. and Berg,C.M. (1994) Inversions and deletions generated by a mini-gamma delta (Tn1000) transposon. *J. Bacteriol.*, **176**, 1332–1338.

Weinert,T.A., Schaus,N.A. and Grindley,N.D. (1983) Insertion sequence duplication in transpositional recombination. *Science*, **222**, 755–765.

Welz,C. (1993) Functionelle analyse des Bakteriellen Insertionelements IS150. PhD thesis, Fakultät für Biologie der Albert-Ludwigs-Univesität Freiburg.

Zerbib,D., Polard,P., Escoubas,J.M., Galas,D. and Chandler,M. (1990a) The regulatory role of the IS1-encoded InsA protein in transposition. *Mol. Microbiol.*, **4**, 471–477.

Zerbib,D., Prentki,P., Gamas,P., Freund,E., Galas,D.J. and Chandler,M. (1990b) Functional organization of the ends of IS1: specific binding site for an IS 1-encoded protein. *Mol. Microbiol.*, **4**, 1477–1486.

Received October 27, 1997; revised and accepted December 3, 1997